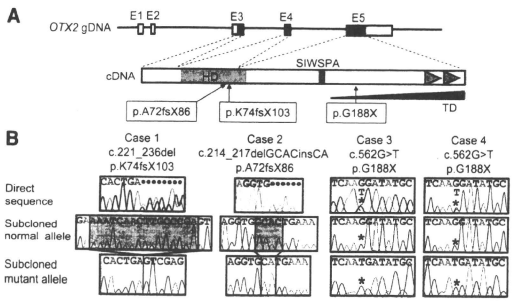

FIG. 1. Sequence analysis in cases 1–4. A, The structure of *OTX2* (the isoform-b) and the position of the mutations identified. The *black* and *white boxes* on genomic DNA (gDNA) denote the coding regions on exons 1-5 (E1-E5) and the untranslated regions, respectively. *OTX2* encodes the HD (a *blue region*), the SIWSPA conserved motif (an *orange region*), and the two tandem tail motifs (*green triangles*). The TD (a *gray triangle*) is assigned to the C-terminal side; deletion of each tail motif reduces the transactivation function, and that of a region distal to the SIWSPA motif further reduces the transactivation function. In addition, another TD may also reside in the 5′ side of the HD (17). The three mutations identified in this study are shown. B, Electrochromatograms showing the mutations in cases 1–4. Shown are the direct sequences and subcloned normal and mutant sequences. The deleted sequences are shaded in *gray*, and the inserted sequence is highlighted in *yellow*. The mutant and the corresponding wild-type nucleotides are indicated by *red asterisks*.

detected by avidin conjugated to fluorescein isothiocyanate. To indicate an extent of a microdeletion, oligoarray comparative genomic hybridization (CGH) was carried out with 1×244K human genome array (catalog no. G4411B; Agilent Technologies, Palo Alto, CA), according to the manufacturer's protocol. Finally, to characterize a microdeletion, long PCR was performed with primer pairs flanking the deleted region, and a long PCR product was subjected to direct sequencing using serial sequence primers. The deletion size and the junction structure were determined by comparing the obtained sequences with the reference sequences at the National Center for Biotechnology Information Database (NC_000014.7; Bethesda, MD), and the presence or absence of repeat sequences around the breakpoints was examined with Repeatmasker (http://www.repeatmasker.org).

Functional studies

Western blot analysis, subcellular localization analysis, DNA binding analysis, and transactivation analysis were performed by the previously reported methods (8) (for details, see Supplemental Methods). In this study, we used the previously reported expression vector and fluorescent vector containing the wild-type *OTX2* cDNA; the probes with the wild-type and mutated OTX2 binding sites within the *IRBP*, *HESX1*, and *POU1F1* promoter sequences; and the luciferase reporter vectors containing the *IRBP*, *HESX1*, and *POU1F1* promoter sequences (8). We further created expression vectors and fluorescent vectors containing mutant *OTX2* cDNAs by site-directed mutagenesis using Prime STAR mutagenesis basal kit (Takara, Otsu, Japan), and constructed a 30-bp probe with wild-type (TAATCT) and mutated (TGGGCT) putative OTX2 binding site within the *GNRH1* promoter sequence and a luciferase reporter vector containing the *GNRH1* promoter sequence (−1349 to −1132 bp) by inserting the corresponding sequence into pGL3 basic. The *GNRH1* promoter sequence was based on the report of Kelley *et al.* (15). Transfections were performed in triplicate within a single experiment, and the experiment was repeated three times.

PCR-based expression analysis of *OTX2*

Human cDNA samples were purchased from CLONTECH (Palo, Alto, CA) except for leukocyte and skin fibroblast cDNA samples that were prepared with Superscript III reverse transcriptase (Invitrogen). PCR amplification was performed for the cDNA samples (0.5 ng), using the primers hybridizing to exon 3 and 4 of *OTX2* and those hybridizing to exons 2/3 and 4/5 (boundaries) of *GAPDH* used as an internal control.

Results

Identification of mutations and substitutions

Three novel heterozygous *OTX2* mutations were identified in four cases, *i.e.* a 16-bp deletion at exon 4 that is predicted to cause a frameshift at the 74th codon for lysine and resultant termination at the 103rd codon (c.221_236del16, p.K74fsX103) in case 1; a 4-bp deletion and a 2-bp insertion at exon 4 that is predicted to cause a frame shift at the 72nd codon for alanine and resultant termination at the 86th codon (c.214_217delGCACinsCA, p.A72fsX86) in case 2; and a nonsense mutation at exon 5 that is predicted to cause a substitution of the 188th glycine with stop codon (c.562G>T, p.G188X) in two unrelated cases (3 and 4; Fig. 1). In addition, heterozygous missense substitutions were identified in patient 1 (c.532A>T, p.T178S) and patient 2 (c.734C>T, p.A245V). Cases 1 and 3 were from group 1, cases 2 and 4 and patient 2 were from group 2, and patient 1 was from group 3. Parental analysis indicated that frameshift mutations in cases 1 and 2 were absent from the parents (*de novo* mutations), whereas the missense substitution of patient 2 was inherited from phenotypically normal father. The parents of cases 3 and 4 and patient 1 refused molecular studies. All the mutations and the missense substitutions were absent from 100 control subjects.

Prediction of the occurrence of aberrant splicing and NMD

The two frameshift mutations and the nonsense mutation were predicted to influence neither exonic splice enhancers nor splice donor and acceptor sites (Supplemental Tables 2 and 3). Furthermore, the two frameshift mutations were predicted to produce the premature termination codons on the mRNA transcribed from the last exon

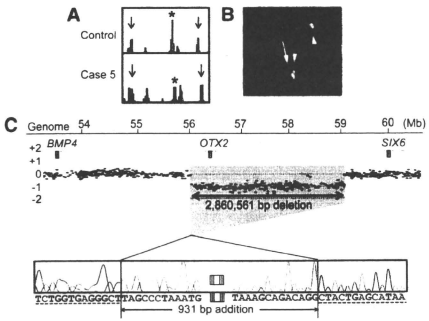

FIG. 2. Deletion analysis in case 5. A, MLPA analysis. The *red asterisk* indicates peaks for the *OTX2* exon 4, and the *black arrows* indicate control peaks. The *red peaks* indicate the internal size markers. Deletion of the MLPA probe binding site is indicated by the reduced peak height. B, FISH analysis. The probe for *OTX2* detects only a *single red signal* (an *arrow*), whereas the RP11-566I2 BAC probe identifies *two green signals* (*arrowheads*). C, Oligoarray CGH analysis and direct sequencing of the deletion junction. The deletion is 2,860,561 bp in physical size (shaded in *gray*) and is associated with an addition of a 931-bp segment (highlighted in *yellow*). The normal sequences flanking the microdeletion are indicated with *dashed underlines*.

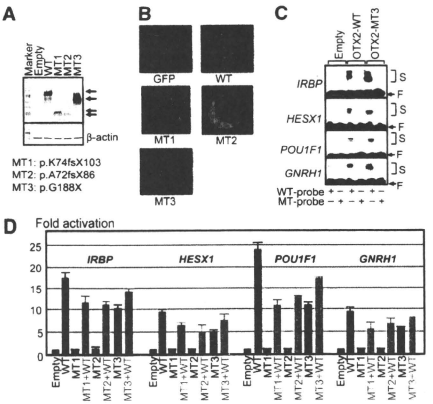

FIG. 3. Functional studies. A, Western blot analysis. Both WT and MT1-MT3 OTX2 proteins are detected with different molecular masses (*arrows*). WT, Wild type; MT1, p.K74fsX103; MT2, p.A72fsX86; and MT3, p.G188X. B, Subcellular localization analysis. Whereas green fluorescent protein (GFP) alone is diffusely distributed throughout the cell, the GFP-fused WT-OTX2 and MT3-OTX2 proteins localize to the nucleus. By contrast, the GFP-fused MT1-OTX2 and MT2-OTX2 proteins are incapable of localizing to the nucleus. C, DNA binding analysis using the wild-type (WT) and mutated (MT) probes derived from the promoters of *IRBP*, *HESX1*, *POU1F1*, and *GNRH1*. The symbols (+) and (−) indicate the presence and absence of the corresponding probes, respectively. Both WT and MT3 OTX2 proteins bind to the WT but not the MT probes. For the probe derived from the *IRBP* promoter, two shifted bands are found for both WT-OTX2 and MT3-OTX2 proteins as reported previously (17). S, Shifted bands; F, free probes. D, Transactivation analysis, using the promoter sequences of *IPBP*, *HESX1*, *POU1F1*, and *GNRH1*. The results are expressed using the mean and SD. The *black*, *blue*, *red*, and *green bars* indicate the data of the empty expression vectors (0.6 μg), expression vectors with WT *OTX2* cDNA (0.6 μg), expression vectors with MT1-MT3 *OTX2* cDNAs (0.6 μg), and the mixture of expression vectors with WT (0.3 μg) and those with MT1-MT3 *OTX2* cDNAs (0.3 μg), respectively; thus, the same amount of expression vectors has been used for each assay.

5, indicating that the frameshift mutations as well as the nonsense mutation had the property to escape NMD (Supplemental Fig. 1).

Identification of a microdeletion

A heterozygous microdeletion affecting *OTX2* was indicated by MLPA and confirmed by FISH in case 5 of group 1 (Fig. 2, A and B). Oligoarray CGH delineated an approximately 2.9-Mb deletion, and sequencing of the fusion point showed that the microdeletion was 2,860,561 bp in physical size (56,006,531–58,867,091 bp on the NC_000014.7) and was associated with an addition of a complex 931-bp segment consisting of the following structures (cen → tel): 2 bp (TA) insertion → 895 bp sequence identical with that in a region just centromeric to the microdeletion (55, 911, 347–55, 912, 241 bp) → 1 bp (C) insertion → 33-bp sequence identical with that within the deleted region (58, 749, 744–58, 749, 776 bp) (Fig. 2C). Repeat sequences were absent around the break points. This microdeletion was not detected in DNA from the parents.

Functional studies of the wild-type and mutant OTX2 proteins

Western blot analysis detected wild-type OTX2 protein of 31.6 kDa and mutant OTX2 proteins of 11.5 kDa (p.K74fsX103), 9.7 kDa (p.A72fsX86), and 15.4 kDa (p.G188X) (Fig. 3A). The molecular masses were as predicted from the mutations. The band intensity was comparable between the wild-type OTX2 protein and the p.G188X-OTX2 protein and was faint for the p.K74fsX103-OTX2 and p.A72fsX86-OTX2 proteins.

Subcellular localization analysis showed that the p.G188X-OTX2 protein localized to the nucleus as did the wild-type OTX2 protein, whereas the p.K74fsX103-OTX2 and p.A72fsX86-OTX2 proteins were incapable of localizing to the nucleus (Fig. 3B). The results were consistent with those of the Western blot analysis because nuclear extracts were used for the Western blotting, with some probable contamination of cytoplasm.

DNA binding analysis revealed that the p.G188X-OTX2 protein with nuclear localizing capacity bound to the wild-type OTX2 binding sites within the four promoters examined, including the *GNRH1* promoter, but not to the mutated OTX2 binding sites (Fig. 3C). The band shift

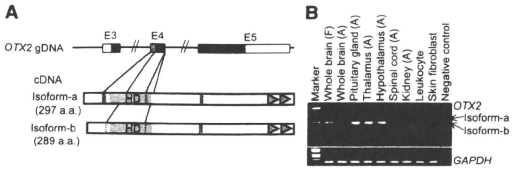

FIG. 4. PCR-based human cDNA library screening for *OTX2* (35 cycles). A, Schematic representation of the *OTX2* isoform-a (NM_21728.2) and isoform-b (NM_172337.1). Because of the two alternative splice acceptor sites at the boundary between intron 3 and exon 4, isoform-a carries eight amino acids (shown in *gray*) in the vicinity of the HD, whereas isoform-b is lacking the eight amino acids. B, PCR amplification data. *OTX2* is clearly expressed in the pituitary and hypothalamus, with isoform-b being the major product. *GAPDH* has been used as an internal control. F, Fetus; A, adult.

was more obvious for the wild-type OTX2 protein than for the p.G188X-OTX2 protein, consistent with the difference in the molecular masses.

Transactivation analysis showed that the wild-type OTX2 protein had transactivation activities for the four promoters examined including the *GNRH1* promoter, whereas the p.K74fsX103-OTX2 and p.A72fsX86-OTX2 proteins had virtually no transactivation function, and the p.G188X-OTX2 protein had reduced (~50%) transactivation activities (Fig. 3D). The three mutant OTX2 proteins had no dominant-negative effects. In addition, the two missense p.A245V-OTX2 and p.T178S-OTX2 proteins had apparently normal transactivation activities with no dominant-negative effect (Supplemental Fig. 2).

PCR-based expression analysis of *OTX2*

OTX2 expression was identified in the pituitary and the hypothalamus as well as in the brain and the thalamus but not detected in the spinal cord, kidney, leukocytes, and skin fibroblasts (Fig. 4). The isoform-b lacking the eight amino acids was predominantly expressed.

Clinical findings in *OTX2* mutation-positive patients

Clinical data are summarized in Table 1 (*left part*). Anophthalmia and/or microphthalmia was present in cases 1–5. Developmental delay was obvious in cases 1 and 3–5, whereas it was obscure in case 2 because of the young age. Prenatal growth was normally preserved in cases 1–5, whereas postnatal growth was compromised in cases 1, 3, and 5. Cases 1 and 5 had IGHD, and case 3 had CPHD (Table 2); furthermore, cases 1, 3, and 5 had pituitary hypoplasia (PH) and/or ectopic posterior pituitary (EPP) (Supplemental Fig. 3). Case 3 showed no pubertal development at 15 yr of age (Tanner pubic hair stage 2 in Japanese boys: 12.5 ± 0.9 yr) (16). Cases 2 and 4 had no discernible pituitary dysfunction and did not receive magnetic resonance imaging examinations. In addition, case 1 had right retractile testis. Patient 1 with p.T178S had CPHD but without ocular anomalies, and patient 2 with p.A245V had bilateral optic nerve hypoplasia and short stature.

Discussion

We identified two frameshift mutations in cases 1 and 2 and a nonsense mutation in unrelated cases 3 and 4. Furthermore, it was predicted that these mutations neither affected splice patterns nor underwent NMD, although direct analysis using mRNA was impossible due to lack of detectable *OTX2* expression in already collected leukocytes as well as skin fibroblasts, which might be available from cases 1–4. Thus, these mutations are predicted to produce aberrant OTX2 proteins *in vivo* that were used in the *in vitro* functional studies. In this context, the functional studies indicated that the two frameshift mutations were amorphic and the nonsense mutation was hypomorphic. The results are consistent with the previous notion that the HD not only has DNA binding capacity but also retains at least a part of nuclear localization signal on its C-terminal portion and the TD primarily resides in the C-terminal region (17) (Fig. 1A). Whereas the two missense substitutions were absent in 100 control subjects, they would be rare normal variations rather than pathological mutations because of the normal transactivation activities with no dominant-negative effect.

We also detected a heterozygous microdeletion involving *OTX2* in case 5 that was not mediated by repeat sequences. This implies the importance of the examination of a microdeletion. Indeed, such a cryptic microdeletion has been identified in multiple genes with the development of MLPA that can serve as a screening method in the detection of microdeletions (18). Whereas the microdeletion of case 5 has removed 16 additional genes (Ensembl Genome Browser, http://www.ensembl.org/), the clinical phenotype of case 5 is explainable by *OTX2* haploinsufficiency alone. Thus, hemizygosity for the 16 genes would not have a major clinical effect, if any.

Furthermore, the present study revealed two findings. First, *OTX2* was expressed in the hypothalamus and had a transactivation function for the *GNRH1* promoter. This implies that *GNRH1* essential for the hypothalamic GnRH secretion is also a target gene of *OTX2*, as has been demonstrated in the mouse (15). Second, the short isoform-b was predominantly identified in the *OTX2* expression-positive tissues. This sug-

TABLE 1. Summary of clinical findings in patients with heterozygous *OTX2* mutations

	Present study					Previous studies[a]			
	Case 1	Case 2	Case 3	Case 4	Case 5	Case 6	Case 7	Case 8	Case 9
Present age (yr)	3	1	15	10	2	3	6	14	6
Sex	Male	Female	Male	Male	Male	Female	Male	Female	Male
Mutation[b]									
cDNA	c.221_236del	c.214_217del GCACinsCA	c.562G>T	c.562G>T	Whole gene deletion	c.402_403insC	c.674A>G	c.674A>G	c.405_406insCT
Protein	p.K74fsX103	p.A72fsX86	p.G188X	p.G188X	Absent	p. S135fsX136	p.N225S	p.N225S	p.S136fsX178
Function	Severe LOF	Severe LOF	Mild LOF	Mild LOF	Absent	Severe LOF	DN	DN	Severe LOF
Ocular malformation									
Right	AO	MO	MO	MO	MO	AO	N.D.	N.D.	AO
Left	MO	MO	MO	MO	AO	AO	N.D.	N.D.	AO
Developmental delay	+	Uncertain	+	+	+	+	N.D.	N.D.	+
Prenatal growth failure[c]	–	–	–	–	–	–	N.D.	N.D.	–
Birth length (cm) (SDS)	46.5 (−1.2)	48.3 (±0)	50 (+0.5)	49 (±0)	47.9 (−0.5)	50 (+0.6)	N.D.	N.D.	49.5 (+0.2)
Birth weight (kg) (SDS)	2.77 (−0.5)	3.22 (+0.6)	3.62 (+1.5)	3.23 (+0.5)	2.96 (−0.1)	3.16 (+0.2)	N.D.	N.D.	3.49 (+1.2)
Birth OFC (cm) (SDS)	32.5 (−0.7)	34 (+0.7)	N.E.	32.5 (−0.7)	31.5 (−1.4)	33.7 (+0.6)	N.D.	N.D.	N.D.
Postnatal growth failure[c]	+	–	+	–	+	+	+	+	+
Present height (cm) (SDS)	76.9 (−3.3)[d]	73.2 (±0)	114.0 (−4.1)[e]	130.8 (−1.5)	78.1 (−2.4)	85.0 (−3.3)	N.D.	N.D.	81.8 (−5.3)[f]
Present weight (kg) (SDS)	8.9 (−2.6)[d]	8.3 (−0.4)	16.8 (−2.4)[e]	23.2 (−1.6)	9.9 (−1.4)	10.1 (−2.6)	N.D.	N.D.	10.7 (−2.5)[f]
Present OFC (cm) (SDS)	N.E.	N.E.	N.E.	N.E.	N.E.	46 (−1.9)	N.D.	N.D.	47.2 (−2.7)[f]
Paternal height (cm) (SDS)[c]	160 (−1.9)	168 (−0.5)	178 (+1.2)	167 (−0.7)	163 (−1.3)	170 (±0)	178 (+0.3)	188 (+1.8)	N.D.
Maternal height (cm) (SDS)[c]	150 (−1.6)	151 (−1.3)	166 (+1.5)	165 (+1.4)	170 (+2.2)	155 (−0.6)	158 (−0.8)	168 (+0.7)	N.D.
Affected pituitary hormones	GH	No	GH, TSH, PRL, LH, FSH	No	GH	GH	GH, TSH, ACTH, LH, FSH	GH, TSH, ACTH, LH, FSH	GH, TSH, ACTH, LH, FSH
MRI findings									
Pituitary hypoplasia	+	N.E.	+	N.E.	+	–	+	+	+
EPP	+	N.E.	+	N.E.	–	–	+	–	+
Other features	Retractile testis (R)			Seizure		Cleft palate			Chiari malformation

SDS, SD score; OFC, occipitofrontal head circumference; MRI, magnetic resonance imaging; LOF, loss of function; DN, dominant negative; AO, anophthalmia; MO, microphthalmia; N.D., not described; N.E., not examined; PRL, prolactin; R, right.

[a] Case 6, Dateki *et al.* (8); cases 7 and 8, Diaczok *et al.* (9); case 9, Tajima *et al.* (10); [b] the cDNA and protein numbes are based on the human *OTX2* isoform-b (GenBank accession no. NM_172337.1), and the A of the ATG encoding the initiator methionine residue is denoted position +1; thus, the description of the mutations in cases 7–9 is different from that reported by Diaczok *et al.* (9) and Tajima *et al.* (10); [c] assessed by the age- and sex-matched Japanese growth standards (27) (cases 1–6 and 9 and their parents) or by the American growth standards (28) (the parents of cases 7 and 8); [d] at 2 yr 4 months of age before GH treatment; [e] at 10 yr of age before GH treatment; [f] at 4 yr of age before GH treatment.

TABLE 2. Blood hormone values in cases 1–5 with heterozygous *OTX2* mutations

Patient		Case 1		Case 2		Case 3		Case 4		Case 5	
Sex (age at examination)		Male (2 yr)		Female (1 yr)		Male (14 yr)		Male (10 yr)		Male (2 yr)	
	Stimulus (dose)	Basal	Peak	Basal	Peak	Basal	Peak	Basal	Peak	Basal	Peak
GH (ng/ml)	Insulin (0.1 U/kg)[a]	1.9[b]	**4.0**[b]	3.3[b]	N.E.	0.8[b]	**1.3**[b]	12.1[b]	N.E.	0.5[c]	**9.0**[c]
	Arginine (0.5 g/kg)									1.1[c]	**7.0**[c]
	L-dopa (10 mg/kg)	1.5[b]	**3.8**[b]			0.3[b]	**1.0**[b]				
LH (mIU/ml)	GnRH (100 μg/m^2)	0.1	1.7	0.1	N.E.	2.3[d]	**4.5**	0.4	N.E.	0.1	3.1
FSH (mIU/ml)	GnRH (100 μg/m^2)	1.0	6.2	3.7	N.E.	1.3[d]	**6.3**	1.1	N.E.	1.5	9.9
TSH (μU/ml)	TRH (10 μg/kg)	4.2	23.8	1.1	N.E.	0.2	**1.9**	1.1	N.E.	5.2	19.5
Prolactin (ng/ml)	TRH (10 μg/kg)	17.9	34.5	N.E.	N.E.	5.5	**8.3**	9.1	N.E.	10.43	88.8
ACTH (pg/ml)	Insulin (0.1 U/kg)	31	195	N.E.	N.E.	24		N.E.	N.E.	41	222
Cortisol (μg/dl)[d]	Insulin (0.1 U/kg)	12.7		9.4	N.E.	19.4		N.E.	N.E.	25.4	39.2
IGF-I (ng/ml)		**8**		65	N.E.	**5**		214	N.E.	48	
Testosterone (ng/dl)		N.E.		N.E.	N.E.	**45**		<5	N.E.	N.E.	
Free T_4 (ng/dl)		1.32		1.17	N.E.	**0.87**		1.15	N.E.	1.17	
Free T_3 (pg/ml)		2.91		3.24	N.E.	**1.94**		3.92	N.E.	4.54	

The conversion factor to the SI unit: GH, 1.0 (μg/liter); LH, 1.0 (IU/liter); FSH, 1.0 (IU/liter); TSH, 1.0 (mIU/liter); prolactin, 1.0 (μg /liter); ACTH, 0.22 (pmol/liter); cortisol, 27.59 (nmol/liter); IGF-I, 0.131 (nmol/liter); testosterone, 0.035 (nmol/liter); free T_4, 12.87 (pmol/liter); and free T_3, 1.54 (pmol/liter). Hormone values have been evaluated by the age- and sex-matched Japanese reference data (29, 30); low hormone data are *boldfaced*. Blood sampling during the provocation tests: 0, 30, 60, 90, and 120 min. N.E., Not examined.

[a] Sufficient hypoglycemic stimulations were obtained during all the insulin provocation tests; [b] GH was measured using the recombinant GH standard, and the peak GH values of 6 and 3 ng/ml are used as the cutoff values for partial and severe GH deficiency, respectively; [c] GH was measured by the classic RIA, and the peak GH values of 10 and 5 ng/ml were used as the cutoff values for partial and severe GH deficiency; [d] Obtained at 0800–0900 h.

gests that the biological functions of *OTX2* are primarily contributed by the short isoform-b.

Clinical features of cases 1–5 are summarized in Table 1, together with those of the previously reported *OTX2* mutation-positive patients examined for detailed pituitary function. Here four patients with cytogenetically recognizable deletions involving *OTX2* are not included (19–22) because the deletions appear to have removed a large number of genes including *BMP4* and/or *SIX6* (Fig. 2B) that can be relevant to pituitary development and/or function (1, 23).

Several points are noteworthy for the clinical findings. First, although cases 1–5 in this study had anophthalmia and/or microphthalmia, ocular phenotype has not been described in cases 7 and 8 identified by *OTX2* mutation analysis in 50 patients with hypopituitarism (9). Whereas no description of a phenotype would not necessarily indicate the lack of the phenotype, *OTX2* mutations may specifically affect pituitary function at least in several patients. This would not be unexpected because several *OTX2* mutation-positive patients are free from ocular anomalies (6).

Second, pituitary phenotype is variable and independent of the *in vitro* function data. This would be explained by the notion that haploinsufficiency of developmental genes is usually associated with a wide range of penetrance and expressivity depending on other genetic and environmental factors (24), although the actual underlying factors remain to be identified. In this regard, because direct mRNA analysis was not performed, it might be possible that the mutations have not produced the predicted aberrant protein and, consequently, *in vitro* function data do not necessarily reflect the *in vivo* functions. Even if this is the case, the quite different pituitary phenotype between cases 3 and 4 with the same mutation would argue for the notion that pituitary phenotype is independent of the residual OTX2 function.

Third, cases 1, 3, 5, and 6–9 with pituitary dysfunction have IGHD or CPHD involving GH, and show the combination of preserved prenatal growth and compromised postnatal growth characteristic of GH deficiency (25). This suggests that GH is the most vulnerable pituitary hormone in *OTX2* mutations. Consistent with this, previously reported patients with ocular anomalies and *OTX2* mutations also frequently exhibit short stature (6, 8). Thus, pituitary function studies are recommended in patients with ocular anomalies and postnatal short stature to allow for appropriate hormone therapies including GH treatment for short stature, cortisol supplementation at a stress period, T_4 supplementation to protect the developmental deterioration, and sex steroid supplementation to induce secondary sexual characteristics. Furthermore, *OTX2* mutation analysis is also recommended in such patients.

Lastly, PH and/or EPP is present in patients with IGHD and CPHD, except for case 6 with IGHD. In this regard, the following findings are noteworthy: 1) heterozygous loss-of-function mutations of *HESX1* are associated with a wide phenotypic spectrum including CPHD, IGHD, and apparently normal phenotype and often cause PH and

EPP, whereas homozygous *HESX1* mutations usually lead to CPHD as well as PH and EPP (2); 2) heterozygous loss-of-function mutations of *POU1F1* usually permit apparently normal pituitary phenotype, whereas homozygous loss-of-function mutations and heterozygous dominant-negative mutations usually result in GH, TSH, and prolactin deficiencies and often cause PH but not EPP (2); and 3) heterozygous *GNRH1* frameshift mutation are free from discernible phenotype, whereas homozygous *GNRH1* mutations result in isolated hypogonadotropic hypogonadism with no abnormal pituitary structure (26). Collectively, overall pituitary phenotype may primarily be ascribed to reduced *HESX1* expression, although reduced *POU1F1* and *GNRH1* expressions would also play a certain role, and there may be other target genes of *OTX2*.

In summary, the results imply that *OTX2* mutations are associated with variable pituitary phenotype, with no genotype-phenotype correlations, and that *OTX2* can transactivate *GNRH1* as well as *HESX1* and *POU1F1*. Further studies will serve to clarify the role of *OTX2* in the pituitary development and function.

Acknowledgments

We thank the patients and parents for participating in this study. We also thank Dr. Nicola Ragge and Dr. David J Bunyan for the MLPA probe sequence of *OTX2*.

Address all correspondence and requests for reprints to: Dr. T. Ogata, Department of Endocrinology and Metabolism, National Research Institute for Child Health and Development, 2-10-1 Ohkura, Setagaya, Tokyo 157-8535, Japan. E-mail: tomogata@nch.go.jp.

This work was supported by Grants-in-Aid for Young Scientists (B-21791025) from the Ministry of Education, Culture, Sports, Science, and Technology and Grants for Child Health and Development (20C-2); Research on Children and Families (H21-005); and Research on Measures for Intractable Diseases (H21-043) from the Ministry of Health, Labor, and Welfare.

Disclosure Summary: The authors have nothing to declare.

References

1. **Cohen LE, Radovick S** 2002 Molecular basis of combined pituitary hormone deficiencies. Endocr Rev 23:431–442
2. **Kelberman D, Dattani MT** 2007 Hypopituitarism oddities: congenital causes. Horm Res 68(Suppl 5):138–144
3. **Vieira TC, Boldarine VT, Abucham J** 2007 Molecular analysis of PROP1, PIT1, HESX1, LHX3, and LHX4 shows high frequency of PROP1 mutations in patients with familial forms of combined pituitary hormone deficiency. Arq Bras Endocrinol Metab 51:1097–1103
4. **Hever AM, Williamson KA, van Heyningen V** 2006 Developmental malformations of the eye: the role of *PAX6*, *SOX2* and *OTX2*. Clin Genet 69:459–470
5. **Courtois V, Chatelain G, Han ZY, Le Novère N, Brun G, Lamonerie T** 2003 New Otx2 mRNA isoforms expressed in the mouse brain. J Neurochem 84:840–853
6. **Ragge NK, Brown AG, Poloschek CM, Lorenz B, Henderson RA, Clarke MP, Russell-Eggitt I, Fielder A, Gerrelli D, Martinez-Barbera JP, Ruddle P, Hurst J, Collin JR, Salt A, Cooper ST, Thompson PJ, Sisodiya SM, Williamson KA, Fitzpatrick DR, van Heyningen V, Hanson IM** 2005 Heterozygous mutations of *OTX2* cause severe ocular malformations. Am J Hum Genet 76:1008–1022
7. **Wyatt A, Bakrania P, Bunyan DJ, Osborne RJ, Crolla JA, Salt A, Ayuso C, Newbury-Ecob R, Abou-Rayyah Y, Collin JR, Robinson D, Ragge N** 2008 Novel heterozygous OTX2 mutations and whole gene deletions in anophthalmia, microphthalmia and coloboma. Hum Mutat 29:E278–E283
8. **Dateki S, Fukami M, Sato N, Muroya K, Adachi M, Ogata T** 2008 OTX2 mutation in a patient with anophthalmia, short stature, and partial growth hormone deficiency: functional studies using the IRBP, HESX1, and POU1F1 promoters. J Clin Endocrinol Metab 93:3697–3702
9. **Diaczok D, Romero C, Zunich J, Marshall I, Radovick S** 2008 A novel dominant-negative mutation of OTX2 associated with combined pituitary hormone deficiency. J Clin Endocrinol Metab 93:4351–4359
10. **Tajima T, Ohtake A, Hoshino M, Amemiya S, Sasaki N, Ishizu K, Fujieda K** 2009 OTX2 loss of function mutation causes anophthalmia and combined pituitary hormone deficiency with a small anterior and ectopic posterior pituitary. J Clin Endocrinol Metab 94:314–319
11. **Cartegni L, Chew SL, Krainer AR** 2002 Listening to silence and understanding nonsense: exonic mutations that affect splicing. Nat Rev Genet 3:285–298
12. **Strachan T, Read AP** 2004 Instability of the human genome: mutation and DNA repair. In: Human molecular genetics. 3rd ed. London and New York: Garland Science; 334–337
13. **Holbrook JA, Neu-Yilik G, Hentze MW, Kulozik AE** 2004 Nonsense-mediated decay approaches the clinic. Nat Genet 36:801–808
14. **Schouten JP, McElgunn CJ, Waaijer R, Zwijnenburg D, Diepvens F, Pals G** 2002 Relative quantification of 40 nucleic acid sequences by multiplex ligation-dependent probe amplification. Nucleic Acids Res 30:e57
15. **Kelley CG, Lavorgna G, Clark ME, Boncinelli E, Mellon PL** 2000 The Otx2 homeoprotein regulates expression from the gonadotropin-releasing hormone proximal promoter. Mol Endocrinol 14:1246–1256
16. **Matsuo N** 1993 Skeletal and sexual maturation in Japanese children. Clin Pediatr Endocrinol 2(Suppl):1–4
17. **Chatelain G, Fossat N, Brun G, Lamonerie T** 2006 Molecular dissection reveals decreased activity and not dominant-negative effect in human OTX2 mutants. J Mol Med 84:604–615
18. **den Dunnen JT, White SJ** 2006 MLPA and MAPH: sensitive detection of deletions and duplications. Curr Protoc Hum Genet Chapter 7, Unit 7.14
19. **Bennett CP, Betts DR, Seller MJ** 1991 Deletion 14q (q22q23) associated with anophthalmia, absent pituitary, and other abnormalities. J Med Genet 28:280–281
20. **Elliott J, Maltby EL, Reynolds B** 1993 A case of deletion 14(q22.1→q22.3) associated with anophthalmia and pituitary abnormalities. J Med Genet 30:251–252
21. **Lemyre E, Lemieux N, Décarie JC, Lambert M** 1998 Del(14)(q22.1q23.2) in a patient with anophthalmia and pituitary hypoplasia. Am J Med Genet 77:162–165
22. **Nolen LD, Amor D, Haywood A, St Heaps L, Willcock C, Mihelec M, Tam P, Billson F, Grigg J, Peters G, Jamieson RV** 2006 Deletion at 14q22–23 indicates a contiguous gene syndrome comprising anophthalmia, pituitary hypoplasia, and ear anomalies. Am J Med Genet A 140:1711–1718

23. **Zhu X, Lin CR, Prefontaine GG, Tollkuhn J, Rosenfeld MG** 2005 Genetic control of pituitary development and hypopituitarism. Curr Opin Genet Dev 15:332–340
24. **Fisher E, Scambler P** 1994 Human haploinsufficiency — one for sorrow, two for joy. Nat Genet 7:5–7
25. **Parks JS, Felner EI** 2007 Hypopituitarism. In: Kliegman RM, Behrman RE, Jenson HB, Stanton BF, eds. Nelson textbook of pediatrics. 18th ed. Philadelphia: Saunders Elsevier; 2293–2299
26. **Bouligand J, Ghervan C, Tello JA, Brailly-Tabard S, Salenave S, Chanson P, Lombès M, Millar RP, Guiochon-Mantel A, Young J** 2009 Isolated familial hypogonadotropic hypogonadism and a GNRH1 mutation. N Engl J Med 360:2742–2748
27. **Suwa S, Tachibana K, Maesaka H, Tanaka T, Yokoya S** 1992 Longitudinal standards for height and height velocity for Japanese children from birth to maturity. Clin Pediatr Endocrinol 1:5–13
28. **Kuczmarski RJ, Ogden CL, Guo SS, Grummer-Strawn LM, Flegal KM, Mei Z, Wei R, Curtin LR, Roche AF, Johnson CL** 2002 2000 CDC growth charts for the United States: methods and development. Vital Health Stat 11 246:1–190
29. **Japan Public Health Association** 1996 Normal biochemical values in Japanese children (in Japanese). Tokyo: Sanko Press
30. **Inada H, Imamura T, Nakajima R** 2002 Manual of endocrine examination for children (in Japanese). Osaka: Medical Review

Mutation and Gene Copy Number Analyses of Six Pituitary Transcription Factor Genes in 71 Patients with Combined Pituitary Hormone Deficiency: Identification of a Single Patient with *LHX4* Deletion

Sumito Dateki, Maki Fukami, Ayumi Uematsu, Masayuki Kaji, Manami Iso, Makoto Ono, Michiyo Mizota, Susumu Yokoya, Katsuaki Motomura, Eiichi Kinoshita, Hiroyuki Moriuchi, and Tsutomu Ogata

Department of Endocrinology and Metabolism (S.D., M.F., M.I., T.O.), National Research Institute for Child Health and Development, Tokyo 157-8535, Japan; Department of Pediatrics (S.D., K.M., E.K., H.M.), Nagasaki University Graduate School of Biomedical Sciences, Nagasaki 852-8501, Japan; Division of Endocrinology and Metabolism (A.U., M.K), Shizuoka Children's Hospital, Shizuoka 232-8555, Japan; Department of Pediatrics and Developmental Biology (M.O.), Tokyo Medical and Dental University Graduate School of Medical and Dental Sciences, Tokyo 113-8519, Japan; Department of Pediatrics (M.M.), Faculty of Medicine, Kagoshima University, Kagoshima 890-8544, Japan; Department of Medical Subspecialties (S.Y.), National Children's Medical Center, Tokyo 157-8535, Japan

Context: Mutations of multiple transcription factor genes involved in pituitary development have been identified in a minor portion of patients with combined pituitary hormone deficiency (CPHD). However, copy number aberrations involving such genes have been poorly investigated in patients with CPHD.

Objective: We aimed to report the results of mutation and gene copy number analyses in patients with CPHD.

Subjects and Methods: Seventy-one Japanese patients with CPHD were examined for mutations and gene copy number aberrations affecting *POU1F1*, *PROP1*, *HESX1*, *LHX3*, *LHX4*, and *SOX3* by PCR-direct sequencing and multiplex ligation-dependent probe amplification. When a deletion was indicated, it was further studied by fluorescence *in situ* hybridization, oligoarray comparative genomic hybridization, and serial sequencing for long PCR products encompassing the deletion junction.

Results: We identified a *de novo* heterozygous 522,009-bp deletion involving *LHX4* in a patient with CPHD (GH, TSH, PRL, LH, and FSH deficiencies), anterior pituitary hypoplasia, ectopic posterior pituitary, and underdeveloped sella turcica. We also identified five novel heterozygous missense substitutions (p.V201I and p.H387P in *LHX4*, p.T63M and p.A322T in *LHX3*, and p.V53L in *SOX3*) that were assessed as rare variants by sequencing analyses for control subjects and available parents and by functional studies and *in silico* analyses.

Conclusions: The results imply the rarity of abnormalities affecting the six genes in patients with CPHD and the significance of the gene copy number analysis in such patients. ***(J Clin Endocrinol Metab* 95: 4043–4047, 2010)**

ISSN Print 0021-972X ISSN Online 1945-7197
Printed in U.S.A.

doi: 10.1210/jc.2010-0150 Received January 20, 2010. Accepted May 13, 2010.
First Published Online June 9, 2010

Abbreviations: CGH, Comparative genomic hybridization; CPHD, combined pituitary hormone deficiency; ESE, exonic splice enhancer; FISH, fluorescence *in situ* hybridization; HPA, hypothalamic-pituitary-adrenal; MLPA, multiplex ligation-dependent probe amplification.

Pituitary development and function depends on spatially and temporally controlled expression of multiple transcription factor genes such as *POU1F1*, *PROP1*, *HESX1*, *LHX3*, *LHX4*, *SOX3*, and *OTX2* (1–3). Mutations of these genes are usually associated with combined pituitary hormone deficiency (CPHD), although they sometimes lead to isolated GH deficiency (1–3). However, mutations of these genes have been found only in a minor portion of patients with CPHD (2–6). Thus, although multiple genes would remain to be identified in CPHD, a certain fraction of mutations may have been overlooked in these known genes. In this regard, because previous studies have primarily been performed with PCR-direct sequencing for coding exons (4–6), gene copy number aberrations (deletions and duplications) affecting such genes, as well as pathological mutations in noncoding regions, may remain undetected in patients with CPHD. Indeed, microdeletions of *PROP1* and *LHX3* and microduplications of *SOX3* have been identified in a few patients with CPHD (7–9). Thus, we performed sequence and gene copy number analyses for six pituitary transcription factor genes in Japanese patients with CPHD.

Patients and Methods

Patients

We studied 71 Japanese patients with various types of CPHD (39 males and 32 females; age 1–43 yr). In all the patients, *OTX2* mutations and gene copy number aberrations have been excluded previously (3).

Primers and probes

The primers and probes used are summarized in Supplemental Table 1 (published on The Endocrine Society's Journals Online web site at http://jcem.endojournals.org).

Sequence analysis

This study was approved by the Institutional Review Board Committee at the National Center for Child Health and Development. After obtaining written informed consent, leukocyte genomic DNA samples of the 71 patients were amplified by PCR for the all coding exons and their flanking splice sites of *POU1F1*, *PROP1*, *HESX1*, *LHX3*, *LHX4*, and *SOX3*. Subsequently, the PCR products were subjected to direct sequencing on a CEQ 8000 autosequencer (Beckman Coulter, Fullerton, CA). To confirm a heterozygous substitution, the corresponding PCR products were subcloned with a TOPO TA cloning kit (Invitrogen, Carlsbad, CA), and normal and mutant alleles were sequenced separately. The GenBank sequence data at NCBI (http://www.ncbi.nlm.nih.gov/genbank) were used as references. For controls, DNA samples of 100 Japanese healthy adults were used with permission.

Functional studies

Functional studies were performed for an *LHX4* missense variant (for details, see Supplemental Methods). In brief, we constructed expression vectors containing wild-type and variant *LHX4* cDNAs and a luciferase reporter vector containing the *POU1F1* promoter sequence with an LHX4-binding site (10). Subsequently, transactivation analysis was performed with dual-luciferase reporter assay system (Promega, Madison, WI) using COS1 cells.

In silico analyses

The conservation status of substituted wild-type amino acid residues was investigated using the UniGene data at NCBI. The possibility that identified substitutions could cause aberrant splicing was examined by ESE finder release 3.0 for the prediction of exonic splice enhancers (ESEs) (http://rulai.cshl.edu/cgi-bin/tools/ESE3/esefinder.cgi) (11) and by the program at Berkeley *Drosophila* Genome Project for the prediction of splice donor and accepter sites (http://www.fruitfly.org/seq_tools/splice.html) (12).

Gene copy number analysis

Muitlplex ligation-dependent probe amplification (MLPA) (13) was performed as a screening of a possible gene copy number alteration (deletion and duplication) in all 71 patients, using a commercially available MLPA probe mix (P236) (MRC-Holland, Amsterdam, The Netherlands) for all coding exons of *POU1F1*, *PROP1*, *HESX1*, *LHX3*, and *LHX4*, together with originally designed probes for *SOX3*. The procedure was as described in the manufacturer's instructions. To confirm a deletion, fluorescence *in situ* hybridization (FISH) was performed with a long PCR product. To indicate an extent of a deletion, oligoarray comparative genomic hybridization (CGH) was carried out with 1x244K Human Genome Array (catalog no. G4411B; Agilent Technologies, Santa Clara, CA), according to the manufacturer's protocol. Finally, to characterize a deletion, long PCR was performed with primer pairs flanking the deleted region, and the PCR product was subjected to direct sequencing using serial sequence primers. The deletion size and the junction structure were determined by comparing the obtained sequences with the reference sequences at NCBI Database (NC_000014.7), and additional deleted genes were examined with Ensembl Database (http://www.ensembl.org/). The presence or absence of repeat sequences around the breakpoints was examined with Repeatmasker (http://www.repeatmasker.org).

Results

Identification of five missense variants

We identified five novel heterozygous missense substitutions, *i.e.* p.T63M (c.188C→T) and p.A322T (c.964G→A) in *LHX3* (GenBank accession number NM_178138), p.V201I (c.601G→A) and p.H387P (c.1160A→C) in *LHX4* (NM_033343), and p.V53L (c.157G→C) in *SOX3* (NM_005634). These substitutions were found in different patients. No other mutations or novel substitutions were identified in the six genes examined. In the 100 control subjects, *LHX4*-p.H387P was detected in four subjects and *SOX3*-p.V53L in three subjects, whereas *LHX3*-p.T63M, *LHX3*-p.A322T, and *LHX4*-p.V201I were absent. Furthermore, sequencing of

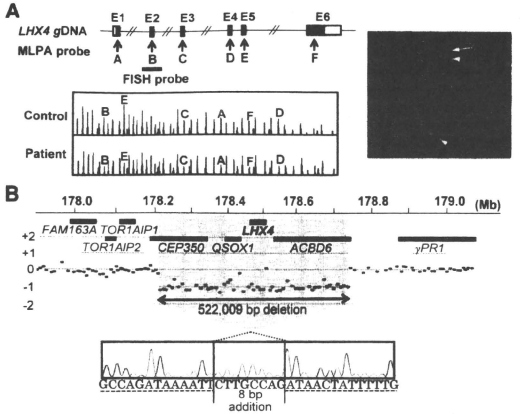

FIG. 1. Gene copy number analysis. Panel A, MLPA and FISH analyses. The *black and white boxes* on genomic DNA (gDNA) denote the coding regions on exons 1–6 (E1–E6) and the untranslated regions, respectively. The sites examined by MLPA probes (A–F) are indicated by *arrows*, and the region identified by the 5305-bp FISH probe is shown by a *thick horizontal line*. In MLPA analysis, the peaks for the sites A–F are reduced in the patient. The *red* peaks indicate the internal size markers. In FISH analysis, the *red* signal is derived from the probe for *LHX4*, and the *green* signals are derived from chromosome 1 centromere control probe (Cytocell, Cambridge, UK) used as an internal control. The probe for *LHX4* is labeled with digoxigenin and detected by rhodamine antidigoxigenin, and the control probe is labeled with biotin and detected by avidin conjugated to fluorescein isothiocyanate. Panel B, Oligoarray CGH analysis and direct sequencing of the deletion junction. The deletion is 522,009 bp in physical size (*shaded in gray*) and is associated with an addition of an 8-bp segment of unknown origin (*highlighted in yellow*). The normal sequences flanking the microdeletion are indicated with *dashed underlines*.

parental samples revealed *LHX3*-p.T63M and *LHX3*-p.A322T in the phenotypically normal mother and father, respectively; parental analysis was refused for *LHX4*-p.V201I, *LHX4*-p.H387P, and *SOX3*-p.V53L. Thus, four missense variants except for *LHX4*-p.V201I were found in healthy controls or parents. For *LHX4*-p.V201I, functional studies showed a normal transactivation function for the *POU1F1* promoter, with no dominant-negative effect (Supplemental Fig. 1). *In silico* analyses indicated that the V201 and the H387 residues in *LHX4* and the A322 residue in *LHX3* were well conserved, whereas the T63 in *LHX3* and the V53 in *SOX3* were poorly conserved (Supplemental Table 2). Furthermore, it was predicted that *LHX4*-V201I and *LHX4*-H387P were unlikely to influence ESEs, whereas *LHX3*-T63M and *LHX3*-A322T might affect ESEs (Supplemental Table 3). None of the missense variants were predicted to influence splice sites (Supplemental Table 4).

Identification of a microdeletion involving *LHX4*

A heterozygous deletion involving *LHX4* was indicated by MLPA and confirmed by FISH (Fig. 1A). Oligoarray CGH and sequencing of the fusion point showed that the deletion was 522,009 bp in physical size and was associated with an addition of an 8-bp segment of unknown origin (Fig. 1B). There were no repeat sequences around the deletion breakpoints. The deletion also affected *CEP350*, *QSOX1*, and *ACBD6*. This microdeletion was absent from the parents.

Patient with the microdeletion

This Japanese female patient was born at 40 wk gestation after an uncomplicated pregnancy and delivery. At birth, her length was 48.0 cm (−0.2 SD), her weight 2.59 kg (−1.0 SD), and her head circumference 33 cm (−0.1 SD). She had transient respiratory distress and hypoglycemia in the early neonatal period. Furthermore, biochemical studies for prolonged jaundice indicated central hypothyroidism at 1 month of age (Table 1). Thus, she was placed on thyroid hormone replacement therapy.

At 1 yr 6 months of age, she was referred to us because of severe short stature. Her height was 64.5 cm (−5.1 SD), and her weight was 6.2 kg (−2.8 SD). Endocrine studies at that time revealed severe GH and prolactin deficiencies (Table 1). Her karyotype was 46,XX in all 50 lymphocytes examined. Recombinant human GH therapy (0.175 mg/kg·wk) was started at 1 yr 8 months of age, showing a remarkable effect. Brain magnetic resonance imaging at 5 yr of age delineated anterior pituitary hypoplasia with a small cystic lesion, ectopic posterior pituitary, and underdeveloped sella turcica (Supplemental Fig. 2). At 11 yr of age, a GnRH test was performed due to lack of pubertal signs, revealing gonadotropin deficiencies (Table 1). Thus, sex steroid replacement therapy was started at 13 yr of age. She had no episode of adrenal insufficiency, with normal blood ACTH and cortisol values at yearly examinations. A CRH stimulation test at 17 yr of age also showed an apparently normal hypothalamic-pituitary-adrenal (HPA) function (Table 1). On the last examination at 17 yr old, she measured 148.7 cm (−1.8 SD), weighed 45.6 kg (−0.9 SD), and manifested full pubertal development. She had no developmental retardation.

The nonconsanguineous parents and the three brothers were clinically normal. The father was 164 cm (−1.2 SD) tall, and the mother was 155 cm (−0.6 SD) tall.

TABLE 1. Blood hormone values of the patient with *LHX4* deletion

			1.5 yr		11 yr		17 yr	
	Stimulus (dosage)	**1 month, basal**	**Basal**	**Peak**	**Basal**	**Peak**	**Basal**	**Peak**
GH (ng/ml)	GHRH (1 mg/kg)		0.2	**1.2**				
	Arginine (0.5 g/kg)		0.1	**0.2**				
	L-Dopa (10 mg/kg)		0.1	**0.1**				
LH (mIU/ml)	GnRH (100 mg/m^2)		<0.5		0.3	**0.8**		
FSH (mIU/ml)	GnRH (100 mg/m^2)		0.5		1.3	**1.6**		
TSH (mU/ml)	TRH (10 mg/kg)	3.5	2.3[a]	**3.9**[a]				
Prolactin (ng/ml)	TRH (10 mg/kg)		**<1.0**	**<1.0**				
ACTH (pg/ml)[b]	CRH (2 mg/kg)		24.6		26.4		26.1	118.7
Cortisol (μg/dl)[b]	CRH (2 mg/kg)		17.5		10.6		15.7	37.82
IGF-I (ng/ml)			**9**					
Free T_4 (ng/dl)		**0.6**	**1.1**[a]					
Estradiol (pg/ml)					**<15**			

The conversion factors to the SI unit are as follows: GH 1.0 (μg/liter), LH 1.0 (IU/liter), FSH 1.0 (IU/liter), TSH 1.0 (mIU/liter), prolactin 1.0 (μg/liter), ACTH 0.22 (pmol/liter), cortisol 27.59 (nmol/liter), IGF-I 0.131 (nmol/liter), free T_4 12.87 (pmol/liter), and estradiol 3.671 (pmol/liter). Hormone values have been evaluated by the age- and sex-matched Japanese reference data; low hormone data are in *bold*. Blood sampling during the provocation tests were done at 0, 30, 60, 90, and 120 min.

[a] Examined under T_4 supplementation therapy.

[b] Obtained at 0800 h.

Discussion

We performed sequence and gene copy number analyses for all coding exons of six previously known genes in 71 patients with CPHD, although noncoding regions were not examined. Consequently, we could identify only a single patient with a heterozygous microdeletion involving *LHX4*. This indicates the rarity of abnormalities affecting the six genes in patients with CPHD and, at the same time, the significance of the gene copy number analysis in such patients. In this regard, because gene copy number aberrations have been found for multiple genes including microdeletions of *PROP1* and *LHX3* and microduplications of *SOX3* (7–9, 14, 15), this implies that gene copy number aberrations should be screened in genetic diagnosis.

Several matters are noteworthy for the clinical and molecular findings of the patient with the microdeletion involving *LHX4*. First, the HPA function was preserved normally at 17 yr of age. However, ACTH deficiency has often been identified in the previously reported patients with heterozygous intragenic loss-of-function mutations of *LHX4* (Supplemental Table 5), and the HPA function often deteriorates with age in patients with CPHD (2). Thus, careful follow-up is necessary for the HPA function of this patient. Second, the microdeletion has affected three additional genes. In this context, the pituitary phenotype of this patient remains within the clinical spectrum of patients with *LHX4* mutations (Supplemental Table 5), and there was no discernible extrapituitary phenotype. Thus, hemizygosity for the three genes would not have a major clinical effect, if any. Third, the deletion breakpoints resided on nonrepeat sequences, and the fusion point was associated with an addition of an 8-bp segment of unknown origin. This indicates that the deletion has been produced by nonhomologous end joining, *i.e.* an aberrant breakage and re-union between nonhomologous sequences (16).

We also identified five novel heterozygous missense substitutions. In this regard, the data obtained from sequencing analysis in control subjects and available parents, functional studies, and *in silico* analyses argue against the five missense substitutions being a disease-causing pathological mutation, although the possibility that they might function as a susceptibility factor for the development of CPHD remains tenable. In particular, *LHX4*-p.V201I, which was absent from 100 control subjects and affected the well-conserved V201 residue, may have been erroneously regarded as a pathological mutation, unless additional studies were performed. Indeed, *LHX4*-p.V201I exerted no predictable effect on the splicing pattern and had a normal transactivation activity in the used system, although transactivation function may be variable depending on the used promoters and cells (17). Such rare variants with an apparently normal function have also been reported previously (3, 18). Thus, whereas *in vitro* experimental data and *in silico* prediction data may not precisely reflect *in vivo* functions, it is recommended to perform such studies for novel substitutions, especially missense substitutions.

In summary, the results imply the rarity of pathological abnormalities in the previously known genes in patients with CPHD and the significance of the gene copy number analysis in such patients. Thus, the causes of CPHD remain elusive in most patients, and additional studies are required to clarify the underlying factors for the development of CPHD.

Acknowledgments

We thank the patients and the parents for participating in this study. We also thank Dr. Takizawa and Dr. Morita for participating in medical care of the reported patients.

Address all correspondence and requests for reprints to: Dr. T. Ogata, Department of Endocrinology and Metabolism, National Research Institute for Child Health and Development, 2-10-1 Ohkura, Setagaya, Tokyo 157-8535, Japan. E-mail: tomogata@nch.go.jp.

This work was supported by Grants for Child Health and Development (20C-2) and Research on Children and Families (H21-005) from the Ministry of Health, Labor, and Welfare and by Grants-in-Aid for Young Scientists (B) (21791025) from the Ministry of Education, Culture, Sports, Science, and Technology, Japan.

Disclosure Summary: All authors report no conflicts of interest.

References

1. **Cohen LE, Radovick S** 2002 Molecular basis of combined pituitary hormone deficiencies. Endocr Rev 23:431–442
2. **Kelberman D, Rizzoti K, Lovell-Badge R, Robinson IC, Dattani MT** 2009 Genetic regulation of pituitary gland development in human and mouse. Endocr Rev 30:790–829
3. **Dateki S, Kosaka K, Hasegawa K, Tanaka H, Azuma N, Yokoya S, Muroya K, Adachi M, Tajima T, Motomura K, Kinoshita E, Moriuchi H, Sato N, Fukami M, Ogata T** 2010 Heterozygous orthodenticle homeobox 2 mutations are associated with variable pituitary phenotype. J Clin Endocrinol Metab 95:756–764
4. **Coya R, Vela A, Pérez de Nanclares G, Rica I, Castaño L, Busturia MA, Martul P; GEDPIT group** 2007 Panhypopituitarism: genetic versus acquired etiological factors. J Pediatr Endocrinol Metab 20: 27–36
5. **Mehta A, Hindmarsh PC, Mehta H, Turton JP, Russell-Eggitt I, Taylor D, Chong WK, Dattani MT** 2009 Congenital hypopituitarism: clinical, molecular and neuroradiological correlates. Clin Endocrinol (Oxf) 71:376–382
6. **Reynaud R, Gueydan M, Saveanu A, Vallette-Kasic S, Enjalbert A, Brue T, Barlier A** 2006 Genetic screening of combined pituitary hormone deficiency: experience in 195 patients. J Clin Endocrinol Metab 91:3329–3336
7. **Abrão MG, Leite MV, Carvalho LR, Billerbeck AE, Nishi MY, Barbosa AS, Martin RM, Arnhold IJ, Mendonca BB** 2006 Combined pituitary hormone deficiency (CPHD) due to a complete PROP1 deletion. Clin Endocrinol (Oxf) 65:294–300
8. **Pfaeffle RW, Savage JJ, Hunter CS, Palme C, Ahlmann M, Kumar P, Bellone J, Schoenau E, Korsch E, Bramswig JH, Stobbe HM, Blum WF, Rhodes SJ** 2007 Four novel mutations of the *LHX3* gene cause combined pituitary hormone deficiencies with or without limited neck rotation. J Clin Endocrinol Metab 92:1909–1919
9. **Woods KS, Cundall M, Turton J, Rizotti K, Mehta A, Palmer R, Wong J, Chong WK, Al-Zyoud M, El-Ali M, Otonkoski T, Martinez-Barbera JP, Thomas PQ, Robinson IC, Lovell-Badge R, Woodward KJ, Dattani MT** 2005 Over- and underdosage of SOX3 is associated with infundibular hypoplasia and hypopituitarism. Am J Hum Genet 76:833–849
10. **Machinis K, Amselem S** 2005 Functional relationship between *LHX4* and *POU1F1* in light of the *LHX4* mutation identified in patients with pituitary defects. J Clin Endocrinol Metab 90:5456–5462
11. **Cartegni L, Chew SL, Krainer AR** 2002 Listening to silence and understanding nonsense: exonic mutations that affect splicing. Nat Rev Genet 3:285–298
12. **Strachan T, Read AP** 2004 Instability of the human genome: mutation and DNA repair. In: Human molecular genetics. 3rd ed. London and New York: Garland Science; 334–337
13. **Schouten JP, McElgunn CJ, Waaijer R, Zwijnenburg D, Diepvens F, Pals G** 2002 Relative quantification of 40 nucleic acid sequences by multiplex ligation-dependent probe amplification. Nucleic Acids Res 30:e57
14. **Desviat LR, Pérez B, Ugarte M** 2006 Identification of exonic deletions in the PAH gene causing phenylketonuria by MLPA analysis. Clin Chim Acta 373:164–167
15. **Fukami M, Dateki S, Kato F, Hasegawa Y, Mochizuki H, Horikawa R, Ogata T** 2008 Identification and characterization of cryptic *SHOX* intragenic deletions in three Japanese patients with Léri-Weill dyschondrosteosis. J Hum Genet 53:454–459
16. **Shaw CJ, Lupski JR** 2004 Implications of human genome architecture for rearrangement-based disorders: the genomic basis of disease. Hum Mol Genet 13:R57–R64
17. **Ito M, Achermann JC, Jameson JL** 2000 A naturally occurring steroidogenic factor-1 mutation exhibits differential binding and activation of target genes. J Biol Chem 275:31708–31714
18. **Castinetti F, Saveanu A, Reynaud R, Quentien MH, Buffin A, Brauner R, Kaffel N, Albarel F, Guedj AM, El Kholy M, Amin M, Enjalbert A, Barlier A, Brue T** 2008 A novel dysfunctional *LHX4* mutation with high phenotypical variability in patients with hypopituitarism. J Clin Endocrinol Metab 93:2790–2799

JMG Online First, published on August 3, 2010 as 10.1136/jmg.2010.079343

Parthenogenetic chimaerism/mosaicism with a Silver-Russell syndrome-like phenotype

K Yamazawa,[1,2] K Nakabayashi,[3] M Kagami,[1] T Sato,[1] S Saitoh,[4] R Horikawa,[5] N Hizuka,[6] T Ogata[1]

► Additional figures, tables and an appendix are published online only. To view these files, please visit the journal online (http://jmg.bmj.com).

[1]Departments of Endocrinology and Metabolism, National Research Institute for Child Health and Development, Tokyo, Japan
[2]Department of Physiology, Development & Neuroscience, University of Cambridge, Cambridge, UK
[3]Maternal-Fetal Biology, National Research Institute for Child Health and Development, Tokyo, Japan
[4]Department of Pediatrics, Hokkaido University Graduate School of Medicine, Sapporo, Japan
[5]Division of Endocrinology and Metabolism, National Children's Hospital, Tokyo, Japan
[6]Department of Medicine, Institute of Clinical Endocrinology, Tokyo Women's Medical University, Tokyo, Japan

Correspondence to
Dr Tsutomu Ogata, Department of Endocrinology and Metabolism, National Research Institute for Child Health and Development, 2-10-1 Ohkura, Setagaya, Tokyo 157-8535, Japan; tomogata@nch.go.jp

Received 20 March 2010
Revised 6 May 2010
Accepted 8 May 2010

ABSTRACT

Introduction We report a 34-year-old Japanese female with a Silver-Russell syndrome (SRS)-like phenotype and a mosaic Turner syndrome karyotype (45,X/46,XX).

Methods/Results Molecular studies including methylation analysis of 17 differentially methylated regions (DMRs) on the autosomes and the *XIST*-DMR on the X chromosome and genome-wide microsatellite analysis for 96 autosomal loci and 30 X chromosomal loci revealed that the 46,XX cell lineage was accompanied by maternal uniparental isodisomy for all chromosomes (upid(AC)mat), whereas the 45,X cell lineage was associated with biparentally derived autosomes and a maternally derived X chromosome. The frequency of the 46,XX upid(AC)mat cells was calculated as 84% in leukocytes, 56% in salivary cells, and 18% in buccal epithelial cells.

Discussion The results imply that a parthenogenetic activation took place around the time of fertilisation of a sperm missing a sex chromosome, resulting in the generation of the upid(AC)mat 46,XX cell lineage by endoreplication of one blastomere containing a female pronucleus and the 45,X cell lineage by union of male and female pronuclei. It is likely that the extent of overall (epi)genetic aberrations exceeded the threshold level for the development of SRS phenotype, but not for the occurrence of other imprinting disorders or recessive Mendelian disorders.

Although a mammal with maternal uniparental disomy for all chromosomes (upd(AC)mat) is incompatible with life because of genomic imprinting,[1] a mammal with a upd(AC)mat cell lineage could be viable in the presence of a co-existing normal cell lineage. In the human, Strain *et al*[2] have reported 46,XX peripheral blood cells with maternal uniparental isodisomy for all chromosomes (upid(AC)mat) in a 1.2-year-old phenotypically male patient with aggressive behaviour, hemifacial hypoplasia and normal birth weight. Because of the 46,XX disorders of sex development, detailed molecular studies were performed, revealing the presence of a normal 46,XY cell lineage in a vast majority of skin fibroblasts and a upid(AC)mat 46,XX cell lineage in nearly all blood cells. In addition, although the data are insufficient to draw a definitive conclusion, Horike *et al*[3] have also identified 46,XX peripheral blood cells with possible upd(AC)mat in a phenotypically male patient through methylation analyses for plural differentially methylated regions (DMRs) in 11 patients with Silver–Russell syndrome (SRS)-like phenotype. This patient was found to have a normal 46,XY cell lineage and a triploid *69,XXY* cell lineage in skin fibroblasts.

However, such patients with a upd(AC)mat cell lineage remain extremely rare, and there is no report describing a human with such a cell lineage in the absence of a normal cell lineage. Here, we report a female patient with a upid(AC)mat 46,XX cell lineage and a non-upd 45,X cell lineage who was identified through genetic screenings of 103 patients with SRS-like phenotype.

MATERIALS AND METHODS

Case report

This Japanese female patient was conceived naturally and born at 40 weeks of gestation by a normal vaginal delivery. At birth, her length was 44.0 cm (−3.1 SD), her weight 2.1 kg (−2.9 SD) and her occipitofrontal head circumference (OFC) 30.5 cm (−2.3 SD). The parents and the younger brother were clinically normal (the father died from a traffic accident).

At 2 years of age, she was referred to us because of growth failure. Her height was 77.7 cm (−2.5 SD), her weight 8.45 kg (−2.6 SD) and her OFC 43.5 cm (−2.5 SD). Physical examination revealed several SRS-like somatic features such as triangular face, right hemihypoplasia and bilateral fifth finger clinodactyly. She also had developmental retardation, with a developmental quotient of 56. Endocrine studies for short stature were normal as were radiological studies. Cytogenetic analysis using lymphocytes indicated a low-grade mosaic Turner syndrome (TS) karyotype, 45,X[3]/46,XX[47]. Thus, a screening of TS phenotype[4] was performed, detecting horseshoe kidney but no body surface features or cardiovascular lesion. Chromosome analysis was repeated at 6 and 32 years of age using lymphocytes, revealing a 45,X[8]/46,XX[92] karyotype and a 45,X[12]/46,XX[88] karyotype, respectively. On the last examination at 34 years of age, her height was 125.0 cm (−6.2 SD), her weight 37.5 kg (−2.0 SD) and her OFC 51.2 cm (−2.8 SD). She was engaged in a simple work and was able to get on her daily life for herself.

Sample preparation

This study was approved by the Institutional Review Board Committees at National Center for Child health and Development. After obtaining written informed consent, genomic DNA was extracted from leukocytes of the patient, the mother and the brother and from salivary cells, which comprise ~40% of buccal epithelial cells and ~60% of leukocytes,[5] of the patient. Lymphocyte metaphase spreads and leukocyte RNA were also

obtained from the patient. Leukocytes of healthy adults and patients with imprinting disorders were utilised for controls.

Primers and probes

The primers utilised in this study are summarised in supplementary methods and supplementary tables 1–3.

DMR analyses

We first performed bio-combined bisulfite restriction analysis (COBRA)[6] and bisulfite sequencing of the *H19*-DMR (A) on chromosome 11p15.5 by the previously described methods[7] and methylation-sensitive PCR analysis of the *MEST*-DMR (A) on chromosome 7q32.2 by the previously described methods[8] with minor modifications (the methylated and unmethylated allele-specific primers were designed to yield PCR products of different sizes, and the PCR products were visualised on the 2100 Bioanalyzer (Agilent, Santa Clara, California, USA)). This was because hypomethylation (epimutation) of the normally methylated *H19*-DMR of paternal origin and maternal uniparental disomy 7 are known to account for 35–65% and 5–10% of SRS patients, respectively.[9 10] In addition, fluorescence in situ hybridisation (FISH) analysis was performed with a ~84-kb RP5-998N23 probe containing the *H19*-DMR (BACPAC Resources Center, Oakland, California, USA). We also examined multiple other DMRs by bio-COBRA. The ratio of methylated clones (the methylation index) was calculated using peak heights of digested and undigested fragments on the 2100 Bioanalyzer using 2100 expert software.

Genome-wide microsatellite analysis

Microsatellite analysis was performed for 96 autosomal loci and 30 X chromosomal loci. The segment encompassing each locus was PCR-amplified, and the PCR product size was determined on the ABI PRISM 310 autosequencer using GeneScan software (Applied Biosystems, Foster City, California, USA).

PCR analysis for Y chromosomal loci

Standard PCR was performed for six Y chromosomal loci. The PCR products were electrophoresed using the 2100 Bioanalyzer.

Expression analysis

Quantitative real-time reverse transcriptase PCR analysis was performed for three paternally expressed genes (*IGF2*, *SNRPN* and *ZAC1*) and four maternally expressed genes (*H19*, *MEG3*, *PHLDA2* and *CDKN1C*) that are known to be variably (usually weakly) expressed in leukocytes (UniGene, http://www.ncbi.nlm.nih.gov/sites/entrez?db=unigene), using an ABI Prism 7000 Sequence Detection System (Applied Biosystems). *TBP* and *GAPDH* were utilised as internal controls.

RESULTS

DMR analyses

In leukocytes, the bio-COBRA indicated severely hypomethylated *H19*-DMR, and bisulfite sequencing combined with *rs2251375* SNP typing for 30 clones revealed maternal origin of 29 hypomethylated clones and non-maternal (paternal) origin of a single methylated clone in this patient (figure 1A). Thus, the marked hypomethylation of the *H19*-DMR was caused by predominance of maternally derived clones rather than hypomethylation of the *H19*-DMR of paternal origin. FISH analysis for 100 lymphocyte metaphase spreads excluded an apparent deletion of the paternally derived *H19*-DMR or duplication of the maternally derived *H19*-DMR (Supplementary figure 1). Methylation-sensitive PCR amplification for the *MEST*-DMR delineated a major peak for the methylated allele and a minor peak for the unmethylated allele (figure 1B). This also indicated the predominance of maternally derived clones and the co-existence of a minor portion of paternally derived clones. Furthermore, autosomal DMRs invariably exhibited markedly abnormal methylation patterns consistent with predominance of maternally inherited DMRs, whereas the methylation index of the *XIST*-DMR on the X chromosome remained within the female reference range (figure 1C). The abnormal methylation patterns were less obvious in salivary cells (thus, in buccal epithelial cells) than in leukocytes, except for the methylation index for the *XIST*-DMR that mildly exceeded the female reference range (figure 1A–C).

Microsatellite analysis

Major peaks consistent with maternal uniparental isodisomy and minor peaks of non-maternal (paternal) origin were identified for at least one locus on each autosome, with the minor peaks of non-maternal origin being more obvious in salivary cells than in leukocytes (figure 1D and supplementary table 4). Furthermore, the frequency of the upid(AC)mat cells was calculated as 84% in leukocytes, 56% in salivary cells and 18% in epithelial buccal cells, using the area under curves for the maternally and the non-maternally inherited peaks (supplementary note). Such minor peaks of non-maternal origin were not detected for all the 30 X chromosomal loci examined.

PCR analysis for Y chromosomal loci

PCR amplification failed to detect any trace of Y chromosome-specific bands in leukocytes and salivary cells (Supplementary figure 2).

Expression analysis

Expression analysis using control leukocytes indicated that, of the seven examined genes, *SNRPN* expression alone was strong enough to allow for a precise assessment (Supplementary figure 3). *SNRPN* expression was extremely low in this patient (figure 1E).

DISCUSSION

These results imply that this patient had a upid(AC)mat 46,XX cell lineage and a non-upd 45,X cell lineage. Indeed, methylation patterns of the *XIST*-DMR is explained by assuming that the two X chromosomes in the upid(AC)mat cells undergo random X-inactivation and that 45,X cells with the methylated *XIST*-DMR on a single active X chromosome[11] are relatively prevalent in buccal epithelial cells. Furthermore, lack of non-maternally derived minor peaks for microsatellite loci on the X chromosome is explained by assuming that the two X chromosomes in the upid(AC)mat cells and the single X chromosome in the 45,X cells are derived from a common X chromosome of maternal origin, with no paternally derived sex chromosome. It is likely, therefore, that a parthenogenetic activation took place around the time of fertilisation of a sperm missing a sex chromosome, resulting in the generation of the 46,XX cell lineage with upid(AC)mat by endoreplication (the replication of DNA without the subsequent completion of mitosis) of one blastomere containing a female pronucleus and the 45,X cell lineage with biparentally derived autosomes and a maternally derived X chromosome by union of male and female pronuclei (figure 2), although it is also possible that a paternally derived sex chromosome was present in the sperm but was lost from the normal

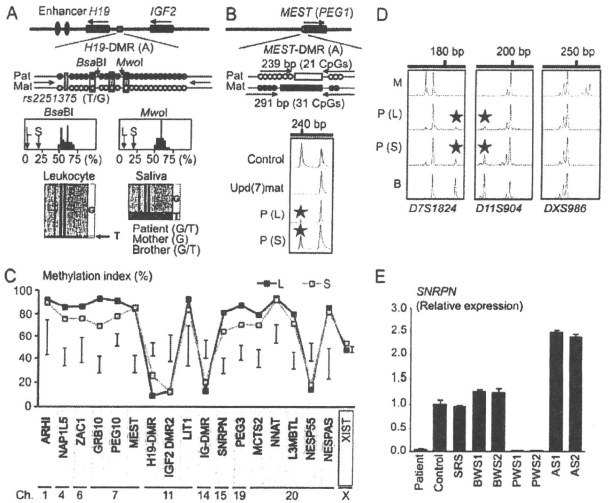

Figure 1 Representative molecular results. Pat, paternally derived allele; Mat, maternally derived allele; P, patient; M, mother; B, brother; L, leukocytes; and S, salivary cells. Filled and open circles in A and B represent methylated and unmethylated cytosine residues at the CpG dinucleotides, respectively. A. Methylation patterns of the *H19*-DMR (A) harbouring 23 CpG dinucleotides and the T/G SNP (*rs2251375*) (a grey box). The PCR products are digested with *Bsa*BI when the cytosine at the sixth CpG dinucleotide (highlighted in yellow) is methylated and with *Mwo*I when the two cytosines at the ninth and the 11th CpG dinucleotides (highlighted in orange) are methylated. For the bio-COBRA data, the black histograms represent the distribution of methylation indices (%) in 50 control participants, and L and S denote the methylation indices for leukocytes and salivary cells of this patient, respectively. For the bisulfite sequencing data, each line indicates a single clone. B. Methylated and unmethylated allele-specific PCR analysis for the *MEST*-DMR (A). In a control participant, the PCR products for methylated and unmethylated alleles are delineated, and the unequal amplification is consistent with a short product being more easily amplified than a long product. In a previously reported patient with upd(7)mat,[8] the methylated allele only is amplified. In this patient, major peaks for the methylated allele and minor peaks for the unmethylated allele (red asterisks) are detected. C. Methylation patterns for the 18 DMRs examined. The DMRs highlighted in blue and pink are methylated after paternal and maternal transmissions, respectively. The black vertical bars indicate the reference data (maximum–minimum) in 20 normal control participants, using leukocyte genomic DNA (for the *XIST*-DMR, 16 female data are shown). D. Representative microsatellite analysis. Minor peaks (red asterisks) have been identified for *D7S1824* and *D11S904* but not for *DXS986* of the patient. Since the peaks for *D7S1824* and *D11S904* are absent in the mother and clearly present in the brother, they are assessed to be of paternal origin. E. Relative expression level (mean ± SD) of *SNRPN* on chromosome 15. The data have been normalised against *TBP*. SRS, an SRS patient with an epimutation (hypomethylation) of the *H19*-DMR; BWS1, a BWS patient with an epimutation (hypermethylation) of the *H19*-DMR; BWS2, a BWS patient with upd(11)pat; PWS1, a PWS patient with upd(15)mat; PWS2, a PWS patient with an epimutation (hypermethylation) of the *SNRPN*-DMR; AS1, an Angelman syndrome (AS) patient with upd(15)pat; and AS2, an AS patient with an epimutation (hypomethylation) of the *SNRPN*-DMR.

cell lineage at the very early developmental stage. Hence, in a strict sense, this patient is neither a chimera resulting from the fusion of two different zygotes nor a mosaic caused by a mitotic error of a single zygote. In this regard, a triploid cell stage is assumed in the generation of a upid(AC)mat cell lineage, and such triploid cells may have been detected in skin fibroblasts of the patient reported by Horike *et al*.[8]

The upid(AC)mat cells accounted for the majority of leukocytes even in adulthood of this patient, despite global negative selective pressure.[12 13] This phenomenon, though intriguing, would not be unexpected in human studies because leukocytes are usually utilised for genetic analyses. Rather, if the upid(AC)mat cells were barely present in leukocytes, they would not have been detected. It is likely, therefore, that upid(AC)mat cells have occupied a relatively large portion of the definitive haematopoietic tissues primarily as a stochastic event. Furthermore, parthenogenetic chimera mouse studies have revealed that parthenogenetic cells are found at a relatively high frequency in some tissues/organs including blood and are barely identified in other tissues/organs such as skeletal muscle and liver.[13] Such a possible tissue-specific selection in favour of the preservation of parthenogenetic cells in the definitive haematopoietic tissues may also be relevant to the predominance of the upid(AC)mat cells in leukocytes. In addition, a reduced growth potential of 45,X cells[14] may also have contributed to the skewed ratio of the two cell lineages.

Clinical features of this patient would be determined by several factors. They include: (1) the ratio of two cell lineages in various tissues/organs, (2) the number of imprinted regions or DMRs relevant to the development of specific imprinting disorders (eg, plural regions/DMRs on chromosomes 7 and 11 for SRS[9 10] and a single region/DMR on chromosome 15 for Prader–Willi syndrome (PWS)),[15] (3) the degree of clinical effects of dysregulated imprinted regions/DMRs (an (epi)dominant effect has been

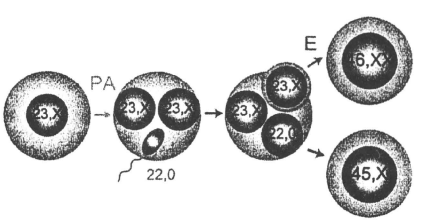

Figure 2 Schematic representation of the generation of the upid(AC) mat 46,XX cell lineage and the non-upd 45,X cell lineage. Polar bodies are not shown. PA, parthenogenetic activation; and E, endoreplication of one blastomere containing a female pronucleus.

assumed for the 11p15.5 imprinted regions including the *IGF2–H19* domain on the basis of SRS or Beckwith–Wiedemann syndrome (BWS) phenotype in patients with multilocus hypomethylation[16] and BWS-like phenotype in patients with a upid (AC)pat cell lineage,[17] a mirror image of a upid(AC)mat cell lineage), (4) expression levels of imprinted genes in upid(AC)mat cells (although *SNRPN* expression of this patient was consistent with upid(AC)mat cells being predominant in leukocytes, complicated expression patterns have been identified for several imprinted genes in androgenetic and parthenogenetic fetal mice, probably because of perturbed *cis*- and *trans*-acting regulatory mechanisms)[18] and (5) unmasking of possible maternally inherited recessive mutation(s) in upid(AC)mat cells.[19] Collectively, it appears that the extent of overall (epi)genetic aberrations exceeded the threshold level for the development of SRS phenotype and horseshoe kidney characteristic of TS[4] but remained below the threshold level for the occurrence of other imprinting disorders or recessive Mendelian disorders.

In summary, we identified a upid(AC)mat 46,XX cell lineage in a woman with an SRS-like phenotype and a 45,X cell lineage accompanied by autosomal haploid sets of biparental origin. This report will facilitate further identification of patients with a upid(AC)mat cell lineage and better clarification of the clinical phenotypes in such patients.

Acknowledgements We thank the patient and her family members for their participation in this study. We also thank Dr. Toshiro Nagai for providing us with blood samples of patients with Prader–Willi syndrome.

Funding This work was supported by grants from the Ministry of Health, Labor, and Welfare and from the Ministry of Education, Science, Sports and Culture.

Competing interests None.

Patient consent Obtained.

Ethics approval This study was conducted with the approval of the Institutional Review Board Committees at National Center for Child health and Development.

Contributors Drs Kazuki Yamazawa (first author) and Kazuhiko Nakabayashi (second author) contributed equally to this work.

Provenance and peer review Not commissioned; externally peer reviewed.

REFERENCES

1. **McGrath J,** Solter D. Completion of mouse embryogenesis requires both the maternal and paternal genomes. *Cell* 1984;**37**:179–83.
2. **Strain L,** Warner JP, Johnston T, Bonthron DT. A human parthenogenetic chimaera. *Nat Genet* 1995;**11**:164–9.
3. **Horike S,** Ferreira JC, Meguro-Horike M, Choufani S, Smith AC, Shuman C, Meschino W, Chitayat D, Zackai E, Scherer SW, Weksberg R. Screening of DNA methylation at the H19 promoter or the distal region of its ICR1 ensures efficient detection of chromosome 11p15 epimutations in Russell–Silver syndrome. *Am J Med Genet Part A* 2009;**149A**:2415–23.
4. **Styne D,** Grumbach M. Puberty: ontogeny, neuroendocrinology, physiology, and disorders. In: Kronenberg H, Melmed M, Polonsky K, Larsen P, eds. *Williams textbook of endocrinology*, 11th edn. Philadelphia: Saunders 2008:969–1166.
5. **Thiede C,** Prange-Krex G, Freiberg-Richter J, Bornhauser M, Ehninger G. Buccal swabs but not mouthwash samples can be used to obtain pretransplant DNA fingerprints from recipients of allogeneic bone marrow transplants. *Bone Marrow Transplant* 2000;**25**:575–7.
6. **Brena RM,** Auer H, Kornacker K, Hackanson B, Raval A, Byrd JC, Plass C. Accurate quantification of DNA methylation using combined bisulfite restriction analysis coupled with the Agilent 2100 Bioanalyzer platform. *Nucleic Acids Res* 2006;**34**:e17.
7. **Yamazawa K,** Kagami M, Nagai T, Kondoh T, Onigata K, Maeyama K, Hasegawa T, Hasegawa Y, Yamazaki T, Mizuno S, Miyoshi Y, Miyagawa S, Horikawa R, Matsuoka K, Ogata T. Molecular and clinical findings and their correlations in Silver–Russell syndrome: implications for a positive role of IGF2 in growth determination and differential imprinting regulation of the IGF2-H19 domain in bodies and placentas. *J Mol Med* 2008;**86**:1171–81.
8. **Yamazawa K,** Kagami M, Ogawa M, Horikawa R, Ogata T. Placental hypoplasia in maternal uniparental disomy for chromosome 7. *Am J Med Genet Part A* 2008;**146A**:514–16.
9. **Abu-Amero S,** Monk D, Frost J, Preece M, Stanier P, Moore GE. The genetic aetiology of Silver–Russell syndrome. *J Med Genet* 2008;**45**:193–9.
10. **Eggermann T,** Eggermann K, Schonherr N. Growth retardation versus overgrowth: Silver–Russell syndrome is genetically opposite to Beckwith–Wiedemann syndrome. *Trends Genet* 2008;**24**:195–204.
11. **Goto T,** Monk M. Regulation of X-chromosome inactivation in development in mice and humans. *Microbiol Mol Biol Rev* 1998;**62**:362–78.
12. **Nagy A,** Sass M, Markkula M. Systematic non-uniform distribution of parthenogenetic cells in adult mouse chimaeras. *Development* 1989;**106**:321–4.
13. **Fundele R,** Norris ML, Barton SC, Reik W, Surani MA. Systematic elimination of parthenogenetic cells in mouse chimeras. *Development* 1989;**105**:29–35.
14. **Verp MS,** Rosinsky B, Le Beau MM, Martin AO, Kaplan R, Wallemark CB, Otano L, Simpson JL. Growth disadvantage of 45, X and 46, X, del(X)(p11) fibroblasts. *Clin Genet* 1988;**33**:277–85.
15. **Horsthemke B,** Wagstaff J. Mechanisms of imprinting of the Prader–Willi/Angelman region. *Am J Med Genet A* 2008;**146A**:2041–52.
16. **Azzi S,** Rossignol S, Steunou V, Sas T, Thibaud N, Danton F, Le Jule M, Heinrichs C, Cabrol S, Gicquel C, Le Bouc Y, Netchine I. Multilocus methylation analysis in a large cohort of 11p15-related foetal growth disorders (Russell Silver and Beckwith Wiedemann syndromes) reveals simultaneous loss of methylation at paternal and maternal imprinted loci. *Hum Mol Genet* 2009;**18**:4724–33.
17. **Wilson M,** Peters G, Bennetts B, McGillivray G, Wu ZH, Poon C, Algar E. The clinical phenotype of mosaicism for genome-wide paternal uniparental disomy: two new reports. *Am J Med Genet Part A* 2008;**146A**:137–48.
18. **Ogawa H,** Wu Q, Komiyama J, Obata Y, Kono T. Disruption of parental-specific expression of imprinted genes in uniparental fetuses. *FEBS Lett* 2006;**580**:5377–84.
19. **Engel E.** A fascination with chromosome rescue in uniparental disomy: Mendelian recessive outlaws and imprinting copyrights infringements. *Eur J Hum Genet* 2006;**14**:1158–69.

RESEARCH LETTER

AMERICAN JOURNAL OF medical genetics

Prenatal Findings of Paternal Uniparental Disomy 14: Delineation of Further Patient

Nobuhiro Suzumori,[1,2]* Tsutomu Ogata,[3] Eita Mizutani,[1,2] Yukio Hattori,[1] Keiko Matsubara,[3] Masayo Kagami,[3] and Mayumi Sugiura-Ogasawara[1]

[1]Department of Obstetrics & Gynecology, Nagoya City University Graduate School of Medicine, Nagoya, Japan

[2]Division of Molecular and Clinical Genetics, Nagoya City University Graduate School of Medicine, Nagoya, Japan

[3]Department of Endocrinology and Metabolism, National Research Institute for Child Health and Development, Tokyo, Japan

Received 5 March 2010; Accepted 2 August 2010

TO THE EDITOR:

Human chromosome 14q32.2 carries a cluster of imprinted genes including paternally expressed genes such as *DLK1* and *RTL1* and maternally expressed genes such as *MEG3* (alias *GTL2*) and *RTL1as* (*RTL1* antisense), together with the germline-derived intergenic differentially methylated region (IG-DMR) and the postfertilization-derived *MEG3*-DMR [da Rocha et al., 2008; Kagami et al., 2008a]. Consistent with this, paternal uniparental disomy 14 (upd(14)pat) results in a unique phenotype characterized by facial abnormality, small bell-shaped thorax with coat-hanger appearance of the ribs, abdominal wall defects, placentomegaly, and polyhydramnios [Kagami et al., 2008a,b], and maternal uniparental disomy 14 (upd(14)mat) leads to less-characteristic but clinically discernible features including growth failure [Kotzot, 2004; Kagami et al., 2008a].

For upd(14)pat, this condition has primarily been identified by the pathognomonic chest roentgenographic findings that are obtained immediately after birth because of severe respiratory dysfunction [Kagami et al., 2008a]. However, upd(14)pat has also been suspected prenatally by fetal radiological findings suggestive of small thorax and other characteristic findings [Curtis et al., 2006; Yamanaka et al., 2010]. Here, we report on prenatal findings in a hitherto unreported upd(14)pat patient. The results will serve to the prenatal identification of similarly affected patients and appropriate neonatal care including respiratory management.

A 41-year-old gravida 1, para 0 Japanese woman was referred to Nagoya City University Hospital because of polyhydramnios at 24 weeks of gestation. The polyhydramnios was severe and required repeated amnioreduction (1,600 ml at 26 weeks, 1,800 ml at 29 weeks, 2,000 ml at 32 weeks, and 2,100 ml at 35 weeks). The fetal urine volume was normal (5–12 ml per hr). At 28 weeks of gestation, 3D ultrasound studies were performed, delineating dysmorphic face, anteverted nares, micrognathia and small thorax characteristic of upd(14)pat (Fig. 1), although the differential diagnosis included Beckwith–Wiedemann syndrome and several types of skeletal dysplasia. Thereafter, ultrasound studies were weekly carried out, indicating almost normal fetal growth and normal umbilical artery Doppler.

How to Cite this Article:
Suzumori N, Ogata T, Mizutani E, Hattori Y, Matsubara K, Kagami M, Sugiura-Ogasawara M. 2010. Prenatal Findings of Paternal Uniparental Disomy 14: Delineation of Further Patient.
Am J Med Genet Part A 152A:3189–3192.

At 37 weeks of gestation, a 2,778 g male infant was delivered by cesarean because of fetal distress. The placenta was 1,384 g (gestational age-matched reference, 510 ± 98 g) [Kagami et al., 2008b]. The patient had severe asphyxia, and immediately received appropriate management including mechanical ventilation for 6 days and nasal directional positive airway pressure at the neonatal intensive care unit. At birth, physical examination revealed hairy forehead, blepharophimosis, depressed nasal bridge, anteverted nares, small ears, protruding philtrum, puckered lips, micrognathia, short webbed neck, joint contractures, and diastasis recti, and roentgenograms showed typical bell-shaped thorax with coat-hanger appearance of the ribs (Fig. 2). Coax valga or kyphoscoliosis was uncertain. Discharge from hospital was 35 days after birth. On the last examination at 8 months of age, the patient

*Correspondence to:
Nobuhiro Suzumori, M.D., Ph.D., Division of Molecular and Clinical Genetics, Department of Obstetrics 8601, Japan.
E-mail: og.n.suz@med.nagoya-cu.ac.jp
Published online 24 November 2010 in Wiley Online Library (wileyonlinelibrary.com)
DOI 10.1002/ajmg.a.33719

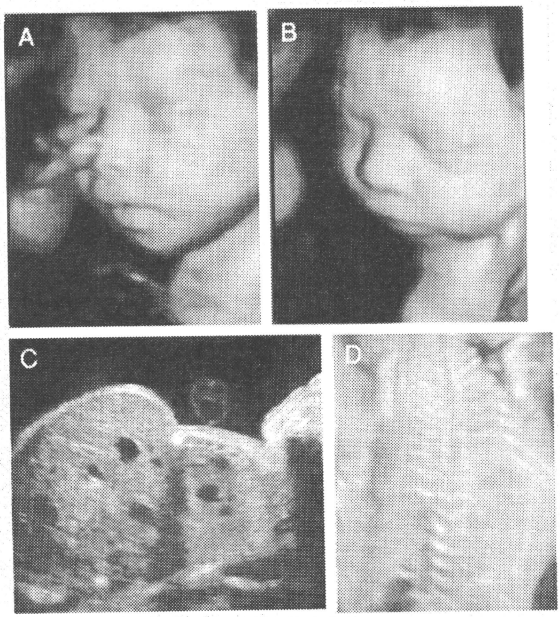

FIG. 1. Prenatal 3D findings at 28 weeks of gestation. A,B: Face appearance with blepharophimosis, depressed nasal bridge, anteverted nares, and micrognathia. C: Small thorax and polyhydramnios. D: Coat-hanger like appearance of the ribs.

required regular oropharyngeal suction and nasogastric tube feeding due to a poor swallowing reflex, and showed developmental delay. At the time of the last evaluation there was no seizure disorder.

To confirm the findings, cytogenetic and molecular studies were performed for the cord blood of the patient by the previously described methods [Kagami et al., 2008a]. This study was approved by the Institutional Review Board Committees at National Center for Child Health and Development and Nagoya City University, and performed after obtaining written informed consent. The karyotype was normal, and metaphase fluorescence in situ hybridization (FISH) analysis with a 202 kb BAC probe containing *DLK1* (RP11-566J3) and a 165 kb BAC probe containing *MG3* and *RTL1/RTL1as* (RP11-123M6) (http://bacpac.-chori.org/) delineated two signals with a similar intensity, respectively. Methylation analysis for bisulfite-treated genomic DNA indicated the presence of paternally derived hypermethylated IG-DMR (CG4 and CG6) and *MEG3*-DMR (CG7) and the absence of maternally derived hypomethylated DMRs. Furthermore, microsatellite analysis was performed using leukocyte genomic DNA of patient and parents, revealing uniparental paternal isodisomy for chromosome 14 (Table I, Fig. 3).

In this patient with molecularly confirmed upd(14)pat, ultrasound studies unequivocally showed typical upd(14)pat phenotypes such as thoracic abnormality and facial dysmorphic features. While this is the first report documenting the facial appearance of the affected fetus, small thorax has been suspected prenatally in five patients with upd(14)pat or epimutations of the IG-DMR and the *MEG3*-DMR, with coat-hanger appearance of the ribs being delineated in one patient [Curtis et al., 2006; Yamanaka et al., 2010]. In this regard, it is notable that polyhydramnios has invariably been identified in upd(14)pat by the second trimester [Kagami et al., 2008a]. It is recommended, therefore, to perform radiological studies for pregnant women with polyhydramnios, to suspect upd(14)pat-compatible clinical features of the fetus. This will permit appropriate counseling and delivery planning at a tertiary

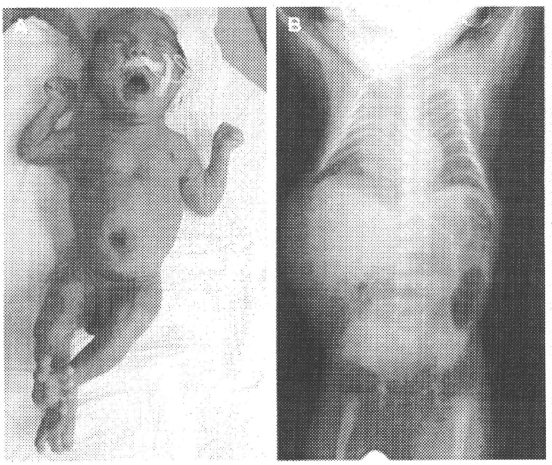

FIG. 2. Postnatal findings at 1 month of age. A: Front view. B: Chest roentgenogram showing bell-shaped thorax with coat-hanger appearance of the ribs.

center with neonatal intensive care as well as pertinent molecular studies using cord blood.

ACKNOWLEDGMENTS

We thank Dr. Saori Kaneko for her assistance in coordinating this research. We also acknowledge the cooperation of the patient's family in allowing us to publish their information.

TABLE I. The Results of Microsatellite Analysis

Locus	Location	Mother	Patient	Father	Assessment
D14S80	14q12	98	98	98	N.I.
D14S608	14q12	200	194	194/210	Isodisomy
D14S588	14q23–24.1	114/126	114	114/122	N.I.
D14S617	14q32.12	139/169	143	143/165	Isodisomy
D14S250	14q32.2	159	159	159/167	N.I.
D14S1006	14q32.2	127/139	127	127/139	N.I.
D14S985	14q32.2	135/137	131	131/133	Isodisomy
D14S1010	14q32.33	134/142	142	142/144	N.I.
D14S1007	14q32.33	119	119	119	N.I.

N.I., not informative.
The Arabic numbers indicate the PCR product sizes in bp.
The imprinted region resides at 14q32.2.
D14S985 is located in the intron of *MEG3*.

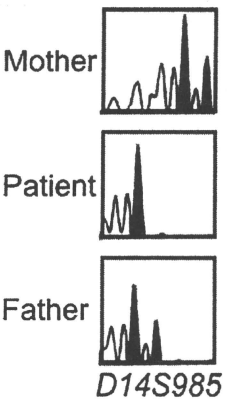

FIG. 3. Microsatellite analysis for *D14S985* residing in the intron of *MEG3*. One of the two peaks in the father is transmitted to the patient, and both of the two peaks in the mother are not inherited by the patient. The PCR fragment size: 135 and 137 bp in the mother, 131 bp in the patient, and 131 and 133 bp in the father. [Color figure can be viewed in the online issue, which is available at wileyonlinelibrary.com]

REFERENCES

Curtis L, Antonelli E, Vial Y, Rimensberger P, Merrer ML, Hinard C, Bottani A, Fokstuen S. 2006. Prenatal diagnostic indicators of paternal uniparental disomy 14. Prenat Diagn 26:662–666.

da Rocha ST, Edwards CA, Ito M, Ogata T, Ferguson-Smith AC. 2008. Genomic imprinting at the mammalian Dlk1-Dio3 domain. Trends Genet 24:306–316.

Kagami M, Sekita Y, Nishimura G, Irie M, Kato F, Okada M, Yamamori S, Kishimoto H, Nakayama M, Tanaka Y, Matsuoka K, Takahashi T, Noguchi M, Tanaka Y, Masumoto K, Utsunomiya T, Kouzan H, Komatsu Y, Ohashi H, Kurosawa K, Kosaki K, Ferguson-Smith AC, Ishino F, Ogata T. 2008a. Deletions and epimutations affecting the human 14q32.2 imprinted region in individuals with paternal and maternal upd(14)-like phenotypes. Nat Genet 40:237–242.

Kagami M, Yamazawa K, Matsubara K, Matsuo N, Ogata T. 2008b. Placentomegaly in paternal uniparental disomy for human chromosome 14. Placenta 29:760–761.

Kotzot D. 2004. Maternal uniparental disomy 14 dissection of the phenotype with respect to rare autosomal recessively inherited traits, trisomy mosaicism, and genomic imprinting. Ann Genet 47: 251–260.

Yamanaka M, Ishikawa H, Saito K, Maruyama Y, Ozawa K, Shibasaki J, Nishimura G, Kurosawa K. 2010. Prenatal findings of paternal uniparental disomy 14: Report of four patients. Am J Med Genet Part A 152A:789–791.